

The genetic relationships between post-traumatic stress disorder and its corresponding neural circuit structures

Qian Gong¹, Honggang Lyu¹, Lijun Kang¹, Simeng Ma¹,
Nan Zhang¹, Xin-hui Xie¹, Enqi Zhou¹, Zipeng Deng¹,
Jiewei Liu^{2*}, Zhongchun Liu^{1,3*}

¹Department of Psychiatry, Renmin Hospital of Wuhan University, 238
Jiefang Road, Wuhan, 430060, Hubei, China.

²Department of Psychiatry, Wuhan Mental Health Center, 89
Gongnongbing Road, Wuhan, 430012, Hubei, China.

³Taikang Center for Life and Medical Sciences, Wuhan University, 115
Donghu Road, Wuhan, 430071, Hubei, China.

*Corresponding author(s). E-mail(s): liujiewei@hust.edu.cn;
zcliu6@whu.edu.cn;

Contributing authors: q1an_gong@whu.edu.cn;

Abstract

Post-traumatic stress disorder (PTSD) may be linked to abnormalities in neural circuits that facilitate fear learning and memory processes. The precise degree to which this connection is influenced by genetic factors is still uncertain. This study aimed to investigate the genetic association between PTSD and its corresponding brain circuitry components. We first conducted a meta-analysis using the summary of PTSD genome-wide association studies (GWAS) from multiple cohorts to enhance statistical power (sample size = 306,400). Then, based on the result of the GWAS meta-analysis, and utilizing the lifetime trauma events (LTE) trait as a control for PTSD, we proceeded with subsequent investigations. We investigated the genetic association of PTSD and LTE with nine brain structure traits related to the brain circuitry by various methodologies, including heritability tissue enrichment analysis, global and local genetic correlations, polygenic overlap analysis, and causal inference. As a result, we discovered an enrichment of heritability for PTSD within circuitry-relevant brain regions such as the cingulate cortex and frontal cortex, alongside the identification of weak genetic correlations

32 between PTSD and these brain regions. We have observed a polygenic overlap
33 between the two trauma-related traits and nine traits of brain circuitry com-
34 ponents such as global cortical area and cingulum. A total of 31 novel jointly
35 significant genetic loci (conjunction FDR < 0.05) associated with PTSD and nine
36 brain structures were identified, suggesting a potential connection between them,
37 and these loci are involved in the process of DNA damage and repair as well as
38 the pathway of neurodegenerative diseases. We also identified a potential causal
39 relationship between PTSD and the surface area of the frontal pole. Our findings
40 offer a valuable understanding of the genetic mechanisms underlying PTSD and
41 its associated brain circuitry.

42 **Keywords:** Post-traumatic stress disorder, neuroimaging traits, genetic correlation

43 1 Introduction

44 Post-traumatic stress disorder (PTSD) is a severe mental disorder that may occur
45 after exposure to traumatic life events. It is characterized by intrusive symptoms,
46 avoidance of trauma-related cues, hyperarousal, negative cognition and moods as the
47 core symptoms.[1] The prevalence of PTSD in the general population is approximately
48 6%. However, people who have experienced various types and degrees of trauma may
49 exhibit higher prevalence rates. For example, war veterans and victims of assault
50 may experience a prevalence of 25% to 35%.[2–4] It has led to serious social burdens,
51 including hospitalizations, suicides and substance abuse.[5] Identifying the mechanisms
52 linked to PTSD would enable the development of interventions to safeguard vulnera-
53 ble groups and address the disorder, thereby alleviating the economic and emotional
54 strain. Prior studies have indicated that the development of PTSD may be associ-
55 ated with abnormalities in brain circuitry that facilitate fear learning and memory
56 mechanisms.[6, 7] The circuit is mainly composed of the amygdala, hippocampus, pre-
57 frontal cortex (PFC) and the connections between them.[6, 7] Researchers suggest that
58 (1) hyperresponsiveness in amygdala is associated with promoting fear associations
59 and expression of fear responses; (2) defects in hippocampal function are associated
60 with mediating deficits in appreciation of safe contexts and explicit learning and mem-
61 ory; and (3) defects in frontal cortex function are associated with mediating deficits
62 in extinction and the capacity to suppress attention or response to trauma-related
63 stimuli.[8, 9]

64 Both animal experiments and neuroimaging studies have validated these views that
65 PTSD is associated with abnormalities in the neural circuits.[8, 10–12] In the neu-
66 ral circuit, amygdala plays a role in fear processing. It was found in rodent studies
67 that sensory information goes first to the basolateral amygdala, where fear learning
68 occurs, and then the signal is transmitted to the central amygdala, which regulates
69 the expression of fear-related behaviors.[13, 14] And in neuroimaging studies, individ-
70 uals with PTSD exhibit heightened activation in the amygdala, which might lead to
71 an overreaction to fear.[15, 16] Hippocampus plays a role in fear acquisition, mem-
72 ory retention, and expression processes, stimulation of which can alter the recall of

fear extinction memory.[17, 18] Researchers have identified reduced hippocampal neurogenesis and dendritic spine loss in the hippocampal CA3 region in trauma-model rodent studies.[19] Meanwhile, neuroimaging studies demonstrate a similar reduction in hippocampal volume among individuals diagnosed with PTSD.[20, 21] PFC plays a role in decision-making and executive functions. Its subregions are associated with suppressing the expression of fear behaviors and the retention of fear extinction memories.[22, 23] This is consistent with reduced gray matter volume and reduced function in the PTSD neuroimaging studies.[24–27] Moreover, the bidirectional communication of the PFC with the hippocampus and amygdala is also important to regulate traumatic fear learning and its extinction.[28] The structural connections between amygdala, hippocampus, and prefrontal structure, specially the microstructure of the cingulum bundle (CG), fornix/stria terminalis (FST), and uncinate fasciculus (UNC), also show abnormalities in patients with PTSD.[29, 30]

The advent of large-scale magnetic resonance imaging (MRI) and genetic datasets has enabled researchers to gain insight into alterations in brain structure and the nexus between disorders and genetic underpinnings.[31] Several twin studies indicate a moderate heritability of brain structure.[32–34] Genome-wide association studies (GWAS) serve as valuable tools for elucidating the genetic mechanisms underlying imaging alterations from a genetic vantage point. Certain single nucleotide polymorphisms (SNPs) identified in these studies delineate factors associated with clinical illness such as schizophrenia, while others delineate risk or protective elements for psychiatric disorders such as neurodevelopment.[35–38]. Consequently, a growing number of studies have begun to focus on the genetic associations and polygenic links between psychiatric disorders and structural brain phenotypes. Most of these studies hypothesized that pleiotropic genes encode risk for mental illness through effects on intermediate or endophenotypes of brain structure.[39–42] This is helpful to quantify the weight of brain traits in the psychiatry disease, discover new loci to complement previous results, and explore the mechanisms by which brain phenotypes act as intermediate or endophenotypes through the biological functions of shared loci.[39–42]

There has been a lack of exploration between PTSD and brain structural studies. By integrating advanced statistical models and the results of large-scale GWAS meta-analyses, it is possible to investigate the genetic overlap between PTSD and brain imaging traits, thereby enhancing the capability to identify associated loci. It is meaningful to study the genetic relationship between PTSD and the neural circuits comprising the amygdala, hippocampus, and PFC and their connections, considering the consistent correlation in clinical symptoms, rodent studies, and neuroimaging studies.[43] Moreover, in GWAS studies of PTSD, the loci identified were also associated with clinical manifestations or risk factors for psychiatric disorders[44, 45], which is consistent with GWAS studies of brain traits as mentioned before. Therefore, we consider that the study of the co-inheritance or polygenicity of PTSD and brain structure traits related to the neurocircuitry can facilitate the identification of new loci and biological mechanisms of PTSD initiation through structural changes in the brain.

In this work, we first combined the GWAS summary data for PTSD from different organizations. We also included lifetime trauma events (LTE) as a control, considering that traumatic events may directly cause changes in brain structure rather than being

118 linked to the development of PTSD. Second, We combined the two trauma-related
119 GWAS summaries with brain cell-type-specific gene expression data to determine if
120 the heritability of trauma-related phenotypes enriches the brain circuits described
121 above. Third, we added GWAS data of brain structure traits (see [Methods](#) for details)
122 to examine the genetic correlations and overlap between trauma-related and them.
123 We use MiXeR[46] to determine the degree of overlapping genetic architecture. We
124 identified risk loci shared between them using the conjunctive false discovery rate
125 (conjFDR)[47] and applied Functional Mapping and Annotation (FUMA) to annotate
126 the identified loci to determine molecular functions of shared risk variants for trauma
127 and brain structure traits.[48] Last, we used bidirectional two-sample Mendelian
128 randomization to investigate the causal relationship between these two types of traits.

129 **2 Methods and Materials**

130 **2.1 GWAS Data and Meta-analysis**

131 GWAS summary data for PTSD was obtained from three large studies: (1) a
132 meta-analysis combining 51 cohorts of European ancestry, including the Psychi-
133 atric Genomics Consortium (PGC, freeze2 PGC-PTSD meta-analysis), and the UK
134 Biobank, encompassing a total of 182,199 samples.[44] (2) Million Veteran Program
135 (MVP, 36,301 cases, 178,107 controls)[49] and (3) FinnGen (2,282 cases, 337,577 con-
136 trols); we utilized liftOver to convert the summary data from the hg38 build to hg37.
137 In the first meta-analysis of 51 cohorts, 19 methods were used to study PTSD, the
138 most common being the Clinician-Administered PTSD Scale and PTSD Checklist,
139 and 91% of participants with PTSD phenotypes were using the PTSD symptom score,
140 while the others used the case/control status.[44] Specific methods of participant and
141 phenotype selection can be found in the original article.[44, 45] PTSD in MVP was
142 a diagnosis of case/control applying the algorithm based on the electronic medical
143 record.[50] PTSD in FinnGen was similarly defined as a case/control status. The meta-
144 analysis of these three summaries was performed using METAL.[51]. We combined
145 p-values across studies taking into account a study specific weight and direction of
146 effect. Risk loci were defined by FUMA[48], using the default parameters.

147 Considering that changes in brain structure may be directly caused by trauma
148 and that there are many people who experience trauma events and do not develop
149 PTSD, we used the GWAS summary for LTE from the UK biobank as a reference.[44]
150 The researchers constructed a count measure of LTE from 8 trauma items of the self-
151 reported retrospective trauma screener from the UKBB mental-health questionnaire.

152 GWAS summary data for cortical was obtained from ENIGMA3 ([https://enigma.
153 ini.usc.edu/](https://enigma.ini.usc.edu/)). It comprised results from 33,992 participants of European ancestry
154 (23,909 from 49 cohorts in the ENIGMA consortium and 10,083 from the UK
155 Biobank).[35] The traits of this study involve the surface area (SA) and thickness
156 (TH) of 34 brain regions of the Desikan-Killiany (DK) atlas. These brain regions were
157 divided according to the gyral-based neuroanatomical regions.[52] According to the
158 radial unit hypothesis, neural progenitor cell proliferation leads to the increase in cor-
159 tical SA, while their neurogenic divisions influence TH.[53] The PFC was not clearly
160 delineated on this atlas, and given the location of the prefrontal lobes and the regions

of the Brodmann area (BA) atlas [54] that we would use in tissue enrichment, we used 161
the frontal poles SA (FSA) and TH (FTH) instead of PFC. In addition, we also con- 162
sidered the relationship between global cortical SA (GSA) and thickness (GTH) and 163
trauma traits. 164

We chose the volume of amygdala (AMY) and hippocampus (HIP) as the subcortical 165
traits. GWAS for the volume of amygdala was from a formal study including 166
53 study samples from the CHARGE consortium, ENIGMA consortium, and UK 167
Biobank.[36] The traits were defined as the mean volume (in cm^3) of the left and 168
right amygdala.[36] Segmentation of brain regions was done according to the freely 169
available and in-house segmentation methods that come with the software used for 170
the different cohorts.[36] GWAS for the volume of hippocampus was obtained from a 171
GWAS study of 33,536 individuals in the ENIGMA Consortium and the CHARGE 172
Consortium.[37] Hippocampal volumes were also estimated using the automated 173
segmentation algorithm in FMRIB Software Library (FSL) and FreeSurfer.[55, 56] 174

GWAS summary data for white matter was obtained from a GWAS of dMRI data 175
from 43,802 individuals across five data resources.[38] This article included 5 DTI indi- 176
cators of 21 white matter pathways. We selected CG, UNC, and FST which are related 177
to PTSD. And we chose fractional anisotropy (FA) as the primary DTI indicator 178
because it has received the most attention in brain white matter research.[57] dMRI 179
measures the directional diffusion of water molecules in tissues, and FA quantifies the 180
degree of directionality, with high FA indicating more organized structures.[57]. 181

The specific locations of the above-mentioned brain areas are shown in Fig 1. 182

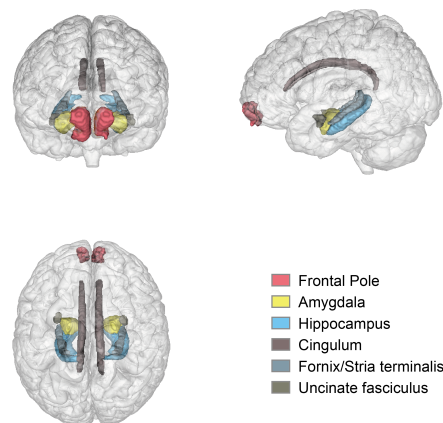


Fig. 1 Brain regions associated with trauma neural circuits mentioned in this article. These brain regions encompass cortical, subcortical structures (amygdala and hippocampus), as well as white matter tracts (cingulum, fornix/stria terminalis, and uncinate fasciculus).

183 2.2 Statistical Analysis

184 2.2.1 Brain tissue enrichment

185 We used linkage-disequilibrium (LD) score regression (LDSC) applied to specifically
186 expressed genes (LDSC-SEG)[58], which tests for enrichment for per-SNP heritability
187 to identify tissue-type-specific enrichment of SNPs. The 13 pre-computed cell-type of
188 brain annotations in GTEx v8 were used in the analysis.[59] A Benjamini-Hochberg
189 false discovery rate (BH-FDR) corrected P value of 0.05 was used as a significant
190 threshold.

191 2.2.2 Global correlations

192 Global correlations were conducted by LDSC[60]. SNPs with high LD exhibit higher
193 χ^2 statistics for polygenic traits compared to SNPs with low LD on average, and a
194 similar pattern arises when replacing the single study statistic with the product of z -
195 scores from two studies with a correlation. We used the calculated LD score from the
196 1000 Gene European population[61] to calculate the global correlation (r_g) between
197 PTSD and brain structure traits. Only SNPs in HAPMAP3 (MAF < 0.01 and INFO
198 > 0.9) were used in the calculation. The range of r_g is between -1 and 1, with -1
199 indicating a perfect negative correlation and 1 indicating a perfect positive correlation.
200 The BH-FDR corrected P value of 0.05 was used as a significant threshold (FDR P
201 < 0.05).

202 2.2.3 Local correlations

203 Local genetic correlations were calculated by Local Analysis of [co]Variant Associa-
204 tion (LAVA).[62] Traditional genetic correlation analysis uses a genome-wide average
205 approach, which may overlook localized genetic contributions and hinder the detection
206 of correlations driven by opposing or heterogeneous effects across the genome. LAVA
207 can estimate genetic relatedness within specific regions of the genome, allowing for
208 inverse correlations between different loci. For LAVA analysis, we followed the protocol
209 described in the original article using the LD reference panel based on 1000 Genomes
210 phase 3 genotype data for European samples,[61, 62] and the partition of the genome
211 into 2495 regions with an average size of 1 Mb. Only regions revealing significant after
212 Bonferroni corrected estimated SNP heritability ($P < 0.05/2495$) in both traits were
213 used to estimate bivariate local genetic correlations between the traits. The BH-FDR
214 corrected P value of 0.05 was used as a significant threshold.

215 2.2.4 Polygenic overlap and shared loci

216 To examine the genetic overlap between pairs of trauma-related phenotypes and brain
217 imaging phenotypes, we used MiXeR v1.3[46] to estimate the overall shared polygenic
218 structure regardless of effect direction and coefficients. To assess polygenic overlap
219 between two traits, MiXeR calculates the overall count of shared and trait-specific
220 causal variants—variants with a non-zero additive genetic effect on a trait. We first
221 performed univariate analysis to derive the number of loci affecting each shape (i.e.,
222 polygenic) and the average magnitude of the additive genetic association between these

variants (i.e., discoverability). Then, a bivariate analysis model was used to estimate 223
the total number of shared and phenotype-specific causal variants. The results of 224
MiXeR are presented as a Venn diagram of shared and unique polygenic components 225
across traits. MiXeR was implemented to calculate the Dice coefficient (i.e., the ratio 226
of shared variants to the total number of variants). The model fit evaluated via the 227
Akaike information criterion (AIC) was based on the maximum likelihood of GWAS 228
z-scores and was illustrated with conditional Q-Q plots. 229

To improve the discovery of specific genetic variants shared between phenotypes, 230
we applied the conditional FDR (condFDR) and conjunction FDR (conjFDR) statis- 231
tical frameworks.[47] condFDR improves the statistical power of association analysis 232
by merging overlapping SNP associations, rearranging association statistics in pri- 233
mary traits according to test statistics for secondary traits, and vice versa.[47, 63] 234
The maximum value between the condFDR for both traits was defined as conjFDR, 235
which provides a conservative estimate for the detection of shared genetic variants. 236
We removed the major histocompatibility complex (MHC) and chromosome 8p23.1 237
genomic regions (hg19, chr6:25,119,106–33,854,733 and chr8:7,242,715–12,483,982) 238
from condFDR analysis to exclude the potential impact of their complex regional LD 239
patterns. A threshold of statistical significance for identifying shared genetic variants 240
was set at conjFDR < 0.05. A locus that did not physically overlap with findings from 241
the original GWAS and the National Human Genome Research Institute-European 242
Bioinformatics Institute (NHGRI-EBI)[64] GWAS Catalog, was considered novel. 243

2.2.5 Functional annotation 244

We apply the FUMA[48] protocol with default parameters to define the independent 245
loci and lead SNPs (conjFDR $P < 0.05$). For all candidate SNPs, which have an 246
LD ($r^2 \geq 0.6$) with at least one of the independent significant SNPs, we conducted 247
functional annotation analysis with the Combined Annotation Dependent Depletion 248
(CADD)[65], RegulomeDB[66], and chromatin states[67]. We performed three gene 249
mapping strategies for candidate SNPs, including positional mapping, expression 250
quantitative trait locus (eQTL) association, and chromatin interaction mapping. We 251
used information from GTEx v8[68] and PsychENCODE[69] to find out the expression 252
of genes we had found. Then, we evaluated the effects' direction of the shared loci by 253
comparing their z-scores and odds ratios. Using Gene2Func in FUMA, we annotated 254
the set of prioritized genes from the first step with biological functions and mecha- 255
nisms. Adjusted P-values with the BH-FDR for multiple test correction methods were 256
computed. 257

2.2.6 Causal relationship 258

To test the potential causal relationship between trauma-related traits and brain 259
structure, we conducted a bidirectional two-sample Mendelian randomization analy- 260
sis. We selected significant independent SNPs (a window size of 1Mb, r^2 threshold 261
of 0.001 and P value threshold of $5e-8$) from the GWAS summary mentioned before 262
as the instrument variants (IVs). We calculate the F-statistics to test the strength of 263
instrument.[70] We used the NHGRI-EBI GWAS catalog[64] and the PhenoScanner 264

265 V2 database[71] to remove SNPs with the confounders and outcome. If an instru-
 266 ment SNP was not available in the outcome GWAS summary, we used LDlinkR[72]
 267 to identify a proxy SNP in LD with the target SNP ($r^2 > 0.8$). We reported the
 268 results for inverse-variance weighted (IVW),[73], weighted median, and MR-Egger
 269 regression.[74, 75] We executed an MR-Egger regression to examine the potential bias
 270 of directional pleiotropy.[75] MR-Pleiotropy Residual Sum and Outlier (MR-PRESSO)
 271 method[76] was applied to detect and correct for horizontal pleiotropy. Last, we per-
 272 formed a leave-one-out analysis where one SNP was removed at a time and IVW was
 273 conducted based on the remaining SNPs.

274 3 Results

275 3.1 GWAS meta-analysis for PTSD

276 To enhance statistical power, we conducted a meta-analysis utilizing three reports
 277 available from multiple cohorts (sample size = 306,400). We identified 16 genome-wide
 278 significant ($P < 5 \times 10^{-8}$) risk loci for PTSD (Table 1 and Fig 2). The LDSC and
 279 quantile-quantile (Q-Q) plots showed that most of the associations were attributed to
 280 polygenicity rather than confounding factors. (intercept, 1.012, s.e., 0.007) (Supple-
 281 mentary Fig. 1). Among these 16 loci, four were reported by the first GWAS summary
 282 about PGC and UKBB[44], and two loci were reported by the second summary about
 283 MVP.[49]

Table 1 Genome-wide significant loci from PTSD GWASs meta analysis.

CHR	rsID	BP	A1	A2	FRQ	Z	P	Reported
1	rs72657988	35688541	T	G	0.083	6.512	7.40E-11	[44]
2	rs6738860	22442099	A	T	0.4611	6.161	7.25E-10	No
2	rs13412865	142547537	T	C	0.4827	5.464	4.65E-08	No
5	rs1875963	155803661	T	G	0.5172	-5.879	4.13E-09	No
6	rs10484538	23468166	T	C	0.0192	5.581	2.40E-08	No
6	rs146918648	28548674	A	G	0.0428	5.922	3.19E-09	[44]
7	rs73046311	1854159	C	G	0.833	5.596	2.19E-08	[49]
7	rs71149745	114056495	A	AAATTTTCAT	0.5679	6.514	7.32E-11	[44]
9	rs4744250	96271752	A	G	0.3454	-5.64	1.70E-08	[44]
11	rs375405046	28710013	CGTGT	C	0.6135	6.038	1.56E-09	[49]
11	rs641325	57681828	T	G	0.3358	6.178	6.48E-10	No
13	rs11617434	67626462	A	G	0.0165	-5.618	1.93E-08	No
15	rs2071382	91428197	T	C	0.4557	-5.941	2.84E-09	No
17	rs12944712	43871147	A	G	0.4522	6.177	6.52E-10	No
17	rs62084750	66085208	T	C	0.7297	-5.746	9.13E-09	No
20	rs6072223	39620847	A	T	0.1587	5.644	1.66E-08	No

A1: the effective allele; FRQ: the frequency of A1; Reported: whether the SNP was reported within 50kb of the loci in the three original summaries.

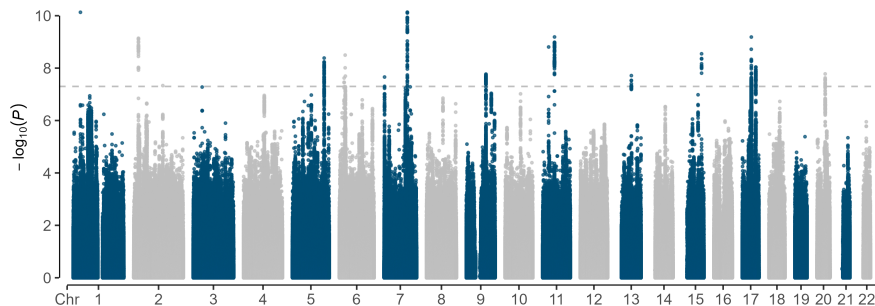


Fig. 2 Manhattan plot for the GWAS meta-analysis. The associations are from the three GWAS meta-analysis. The gray line shows the genome-wide significant P threshold ($P < 5 \times 10^{-8}$).

3.2 The tissue enrichment of heritability aligned with circuitry structure 284 285

To identify tissue types that are more likely to be involved in the neural circuit of 286 trauma, we used the trauma-related GWAS summary statistics and 13 brain tissue 287 type-specific data from GTEx v8 by LDSC-SEG. We found that the expression of 288 PTSD loci was enriched in “Brain Anterior cingulate cortex (BA24)” ($P_{FDR} = 0.0012$), 289 “Brain Frontal Cortex (BA9)” ($P_{FDR} = 0.0019$), and “Brain Cortex” ($P_{FDR} = 0.013$), 290 while the expression of LTE loci was enriched in “Brain Cortex” ($P = 0.009$, not 291 significant after adjustment) (Supplementary Table 1). The results are consistent with 292 the brain areas we mentioned earlier. 293

3.3 Global and local genetic correlations 294

We estimated the global genetic correlation using LDSC between trauma-related and 295 brain structure-related traits. The results showed weak correlation between PTSD 296 and GSA ($r_g = -0.0901$, $P = 0.018$), LTE and FST ($r_g = -0.1301$, $P = 0.0035$), 297 LTE and CG ($r_g = -0.1038$, $P = 0.0224$). The results were not significant after FDR 298 (Supplementary Table 2). 299

Local genetic correlation may be overridden in the calculation of r_g , so we used 300 LAVA to estimate the local genetic correlations. LAVA local correlations provided 301 further evidence of the relationship between trauma and brain structure. Loci with a 302 significant amount of local genetic signal for both traits ($P < 0.05/2495$) were used in 303 the bivariate analysis. PTSD is significantly correlated with the local genetic variations 304 in GSA ($n = 4$), GTH ($n = 1$), FSA ($n = 3$), AMY ($n = 3$), HIP ($n = 5$), CG ($n = 6$), 305 FST ($n = 7$), and UNC ($n = 4$). The number of loci demonstrating a significant local 306 correlation between LTE and brain structure is fewer than those observed in PTSD. 307 The results between LTE and brain structure were as follows: GTH ($n = 1$), CG ($n = 308$ 2), and UNC ($n = 2$). Especially, the region in chr7: 155280611-156344386 is significant 309 in both PTSD-GSA and PTSD-hippocampus pairs, and the region in chr17: 43460501- 310 44865832 is significant in both PTSD-GSA and PTSD-FST. (Supplementary Table 311 3). 312

313 3.4 Shared genomic architectures and loci between 314 trauma-related traits and brain structure-related traits

315 Univariate MiXeR estimated the SNP heritability (h^2) to be 0.049 for PTSD and
316 0.066 for LTE. The h^2 of brain structure estimated by MiXeR ranged from 0.0041
317 to 0.32. The results of trait-influencing variants showed that trauma-related traits
318 were 3-4 times more polygenic than brain structure, with 10K and 7.8K variants
319 relative to PTSD and LTE, while there were only 3.2K variants related to GTH,
320 which was the most polygenic brain structure-related phenotype. (Supplementary Fig.
321 2 and Supplementary Table 4). Bivariate MiXeR revealed significant polygenic overlap
322 between brain structure-related variants and trauma-related variants. The UNC shared
323 the largest proportion of trait-influencing variants with PTSD (98%, 2008 out of 2059),
324 and the GSA shared the largest proportion of trait-influencing variants with LTE
325 (96%, 1751 out of 1820). (Fig 3) Among the pairs of PTSD, the results of GSA, GTH,
326 CG, FST, and UNC can also be further supported by AIC values and Q-Q diagrams
327 (Supplementary Fig. 3). All the results can be found in Supplementary Table 5.

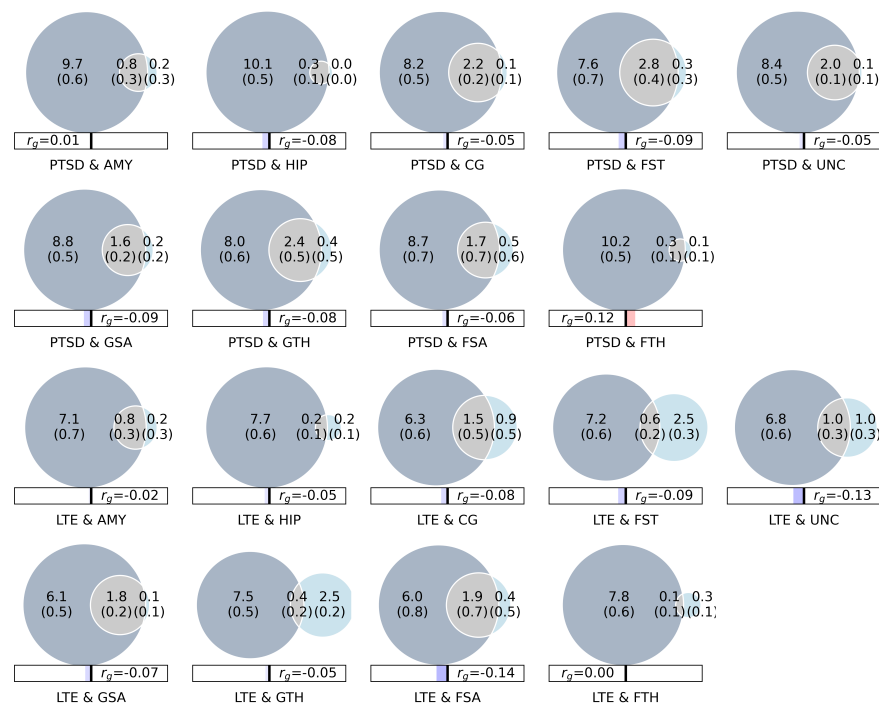


Fig. 3 Polygenic overlap between trauma-related traits and brain structure-related traits The Venn diagram shows the estimated number of causal variants shared between trauma-related traits and brain structure-related traits. The number of causal variants in thousands is shown, as well as the standard error. Abbreviations: PTSD, post-traumatic stress disorder; LTE, lifetime trauma events; GSA, global cortical surface area; GTH, global cortical thickness; FSA, frontal poles surface area; FTH, frontal poles thickness; AMY: amygdala; HIP: hippocampus; CG: cingulum bundle; FST: fornix/stria terminalis; UNC: uncinate fasciculus.

To explore the genetic sharing of trauma-related traits and brain structure-related traits, we applied conjFDR analysis for each pair. We discovered 40 independent loci that were jointly associated with PTSD with conjFDR < 0.05, including 12 loci for GSA, 7 loci for GTH, 1 locus for FSA, 2 loci for FTH, 1 locus for AMY, 4 loci for HIP, 11 loci for CG, 1 locus for FST, and 2 loci for UNC (Fig 4 and Table 2). In particular, one locus (lead SNP rs2352974, chr3:49734229-50176259) was associated in both CG and UNC with PTSD. There were only 9 loci that were jointly associated with LTE with conjFDR < 0.05. Therefore, in the subsequent functional analysis, we will only show PTSD-related results. Among those 40 PTSD risk loci identified by leveraging GWAS of brain structural traits, 31 lead SNPs that had not been reported as significant in the previous PTSD GWAS studies were defined as novel. See Supplementary Table 6 for details.

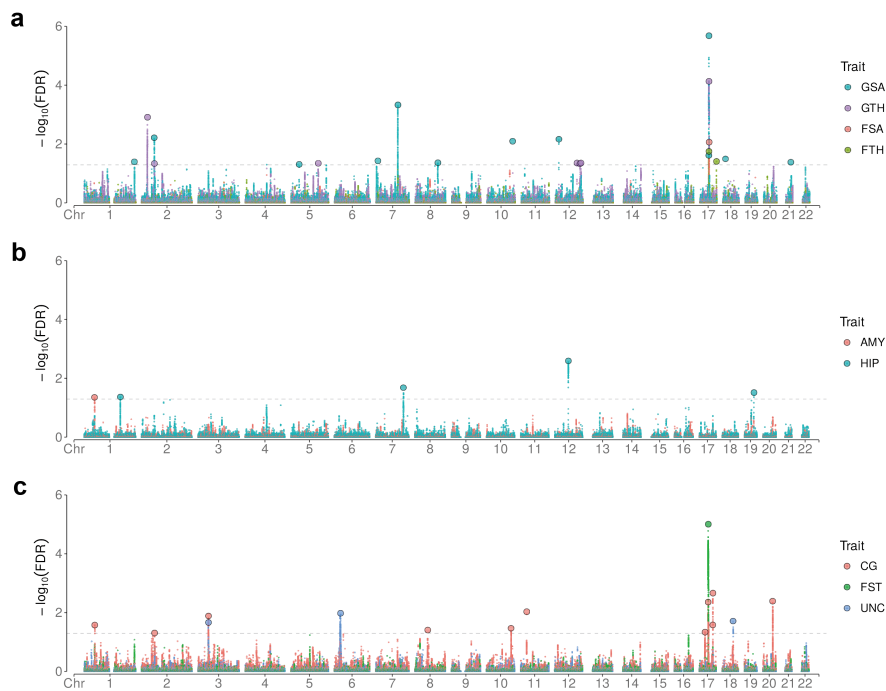


Fig. 4 Chromosomal distribution of genetic loci jointly associated with PTSD and brain structure-related traits. The Manhattan plots show the common genetic variants jointly associated with PTSD and brain structure traits at conjFDR < 0.05. **a.** Results between PTSD and cortical traits. **b.** Results between PTSD and subcortical traits. **c.** Results between PTSD and white matter traits. Further details are provided in Table 2 and Supplementary Table 6-9. Abbreviations: GSA, global cortical surface area; GTH, global cortical thickness; FSA, frontal poles surface area; FTH, frontal poles thickness; AMY: amygdala; HIP: hippocampus; CG: cingulum bundle; FST: fornix/stria terminalis; UNC: uncinate fasciculus.

Table 2 Lead genomic loci significantly associated with PTSD and brain structural traits at a conjFDR < 0.05.

Brain_trait	locus	CHR	LEAD_SNP	LEAD_BP	MimBP	MaxBP	FDR	nearestGene	P_PTSD	Z_PTSD	P_brain	Z_brain	ConcordEffect	Novel	
GSA	1	1	rs58594024	243674094	243674094	60528052	0.006107	AKT3	0.000168	-3.763	2.77E-05	4.19146	No	Yes	
	2	5	rs955658	60501421	60405620	60528052	0.004107	AC007381.3	1.44E-05	-4.337	4.35E-05	4.08827	No	Yes	
	3	5	rs10057563	39081519	39081519	60528052	0.049359	RICTOR	0.000223	3.692	6.92E-05	-3.97907	No	Yes	
	4	7	rs2058277	8132877	8133389	8133389	0.007309	SLC6A11	0.000151	3.79	0.00045	3.50883	Yes	Yes	
	5	7	rs9649275	104935801	104579775	105078345	0.000047	SRPK2	5.15E-07	5.021	5.06E-06	4.5624	Yes	Yes	
	6	8	rs76740786	109172043	109063823	109243959	0.043365	AP001331.1	0.000181	3.744	0.000704	-3.38822	No	Yes	
	7	10	rs61753077	123996970	123996970	123996970	0.000857	TACC2	9.06E-07	-4.911	0.0001	-3.88959	Yes	Yes	
	8	12	rs9651873	16755372	16743217	16756508	0.000871	MGST1-LMO3	1.68E-05	4.304	7.96E-05	-3.94576	No	Yes	
	9	17	rs11652522	43055579	43055579	43055579	0.024487	CTD-253421.9	8.38E-05	3.933	0.000353	-3.57313	No	Yes	
	10*	17	rs12944712	43871147	43460181	44865603	2.10E-06	CRHR1-RP11-105N13.4	6.52E-10	6.177	4.80E-10	-6.22542	No	No	
	11	18	rs4797662	12268928	12267865	12268928	0.032144	CIDEA	0.000123	-3.839	0.000312	-3.6055	Yes	Yes	
	12	21	rs4817863	38824655	38715469	38902521	0.041578	DYRK1A	0.000161	-3.773	0.000667	-3.40263	Yes	Yes	
GTH	1	2	rs7605526	27345484	26961166	27351279	0.001241	ABHD11	1.67E-06	-4.79	6.30E-07	4.875	No	Yes	
	2	2	rs7583383	61500322	61387298	61500322	0.046248	USP34	0.000135	-3.818	3.16E-05	-4	Yes	Yes	
	3	5	rs247008	131447104	131447104	131447104	0.045386	smoZ6	0.000131	-3.824	2.40E-05	-4.125	Yes	Yes	
	4	12	rs10778315	104667244	104655942	104670449	0.044259	TXNRD1-RP11-818F20.5	0.000127	-3.832	0.000138	4	No	Yes	
	5	12	rs795483	118590579	118580315	118830958	0.046765	TAOK3	3.54E-05	-4.135	0.000501	-3.375	No	Yes	
FSA	6	12	rs7132277	123593382	123450765	123913433	0.044333	PITPNM2	0.000127	-3.832	0.000132	-3.6	Yes	Yes	
	7	17	rs2316767	43919070	43460181	44865603	7.41E-05	MAPT-AS1	4.71E-08	-5.462	2.90E-10	-6.27273	Yes	No	
	8	17	rs79730878	43849415	43463493	44848517	0.017819	NSF	1.44E-06	-4.819	2.26E-05	-4.23743	Yes	No	
	9	17	rs9912348	79959669	79921061	79981316	0.038966	ASPSCR1	8.57E-08	-5.355	5.07E-05	-4	Yes	No	
	10	17	rs11588333	51236592	50891093	5126458	0.044327	FAFI	9.47E-05	3.904	0.00012	-3.84211	No	Yes	
	11	17	rs71645275	176192961	175908200	176416712	0.042928	RP11-195C7.1	4.63E-05	4.074	1.24E-05	-4.37116	No	Yes	
	12	7	rs2346449	133733917	133623791	133733917	0.020799	EXOC4	9.40E-05	3.905	3.10E-05	4.166	Yes	Yes	
	3	12	rs1244796	65159137	65100884	65236019	0.002569	RP11-629N8.3	2.40E-06	4.716	4.06E-06	-4.608	No	Yes	
	4	19	rs483082	45416178	45396665	45418790	0.030551	APOC1	5.94E-05	4.015	0.000177	-3.75	No	Yes	
	1	1	rs7413471	52339759	52266242	52406432	0.026767	NRD1	4.82E-05	-4.064	6.34E-06	-4.51482	Yes	Yes	
	2	2	rs144003047	62835070	62835070	63287328	0.049509	AC092155.4	0.000117	-3.852	0.000266	-3.64596	Yes	Yes	
	3	3	rs2352974	49890613	49734229	50176259	0.013003	TRAP1	1.90E-05	4.276	1.30E-06	4.83915	Yes	Yes	
CG	4	8	rs597123	61572983	61396829	61588391	0.039262	RP11-9120.1	8.25E-05	3.937	0.000112	-3.86202	No	Yes	
	5	10	rs35276948	118786704	118648043	118896767	0.034242	KIAA1598	6.79E-05	3.983	4.91E-05	4.05972	Yes	Yes	
	6	11	rs3076902	28671055	28591168	28709434	0.009933	RP11-960D24.1	3.81E-07	-5.078	4.50E-05	4.08003	No	No	
	7	17	rs3098948	27970522	27985546	28553639	0.046187	MAPT-AS1	0.000105	3.879	1.83E-06	-4.77129	No	Yes	
	8	17	rs6503451	43948347	43460181	44865498	0.004411	HELZ	5.27E-06	-4.554	1.00E-05	-4.34251	No	No	
	9	17	rs5821488	65123957	65089727	65263650	0.026517	KPNA2	1.44E-06	-4.819	0.000182	-3.74252	Yes	Yes	
	10	17	rs62086003	66016006	65825248	66204635	0.002178	MAPT-AS1	1.24E-06	-4.848	6.32E-06	-4.51537	No	No	
	11	20	rs35888516	47764275	47508077	47935069	0.004093	STAU1	3.66E-06	4.63	1.46E-05	-4.33446	No	No	
	1*	1	rs111825734	44019107	43460181	44865498	9.99E-06	MAPT	5.02E-09	-5.846	2.85E-12	-6.98507	No	No	
	UNC	1	3	rs2352974	49890613	49734229	49960388	0.021753	TRAP1	1.90E-05	4.276	6.12E-05	-4.00814	No	Yes
		2	18	rs6566169	53301527	53197944	53389061	0.019584	TCF4	1.79E-05	-4.29	1.40E-05	-4.34391	Yes	Yes

* Loci with significant local genetic correlation.

3.5 Functional annotation and gene-set analysis 340

Functional annotation for all shared lead SNPs identified in conjFDR between PTSD 341 and brain structure analysis showed that 76% were intergenic or intronic, while only 342 1 lead SNP was exonic and 8 SNPs were associated with noncoding-RNA. Four lead 343 SNPs (rs955658, rs9651873, rs199439, and rs7413471) had a CADD score above the 344 threshold score of 12.37, indicative of deleteriousness. Two of these were associated 345 with GSA and showed opposite effects in PTSD and GSA, which was consistent with 346 the conclusions of basic research. Moreover, 5 lead SNPs displayed “1f” in the RDB 347 score, which means they were likely to affect binding and be linked to the expression 348 of a gene target. Functional annotation for all SNPs in the loci shared between PTSD 349 and brain structure (conjFDR < 0.05) displayed that 60.2% of them were intronic or 350 intergenic (1692 of 2810), 1.4% were exonic (40 of 2810), and 33.9% were associated 351 with noncoding-RNA (953 of 2810). 352

We applied FUMA to link the candidate SNPs ($r^2 \geq 0.6$) of 40 shared lead loci to 353 1,426 genes. It is worth noting that genes MAPT-AS1, SPPL2C, and CRHR1 could 354 be annotated in all three ways and were related to five or more structure traits. These 355 three genes were all located on chromosome 17. (Supplementary Table 7-10) Gene-set 356 analysis of Gene Ontology (GO) for genes indicated by all SNPs in the loci shared 357 between PTSD and brain structure, respectively, showed significantly associated 6 358 biological processes, 4 cellular components, and 8 molecular functions. (Supplementary 359 Table 11) 360

3.6 Positive causal relationship from PTSD to FSA 361

We used bidirectional Mendelian randomization to explore whether the genetic over- 362 lap between two phenotypes suggests a causal relationship. Among all phenotype 363 pairs, we only found a significant and consistent causal relationship from PTSD to 364 FSA using 3 of 5 MR methods. (Fig 5). No obvious heterogeneity was detected in 365 genetic variants associated with PTSD and FSA (Cochran’s Q = 10.18 and $P = 0.60$). 366 The IVW method showed that genetically predicted higher PTSD risk was related to 367 FSA (β 13.01; 95% CI, 4.49 to 21.53; $P = 0.003$). MR-RAPs and weighted median 368 both demonstrated the effect of PTSD on FSA and provided evidence of the stabil- 369 ity of the results of the IVW method. The results among other traits are detailed in 370 Supplementary Table 12. 371

The scatter plots of SNP potential effects on PTSD versus FSA were demonstrated 372 in Supplementary Fig. 4, with the slope of each representing the evaluated effect size 373 per method. Among the 13 SNPs, only rs641325 was related to increased risks of 374 PTSD and FSA. The result of the LOO analysis was presented in Supplementary Fig. 375 5, where no single SNP was driving the whole effect. 376

4 Discussion 377

In this study, we first conducted a meta-analysis on three accessible large-scale GWAS 378 datasets, revealing 10 novel loci that were not identified in any of the three individ- 379 ual studies to enhance the statistical power. Then we utilized a series of genetically 380

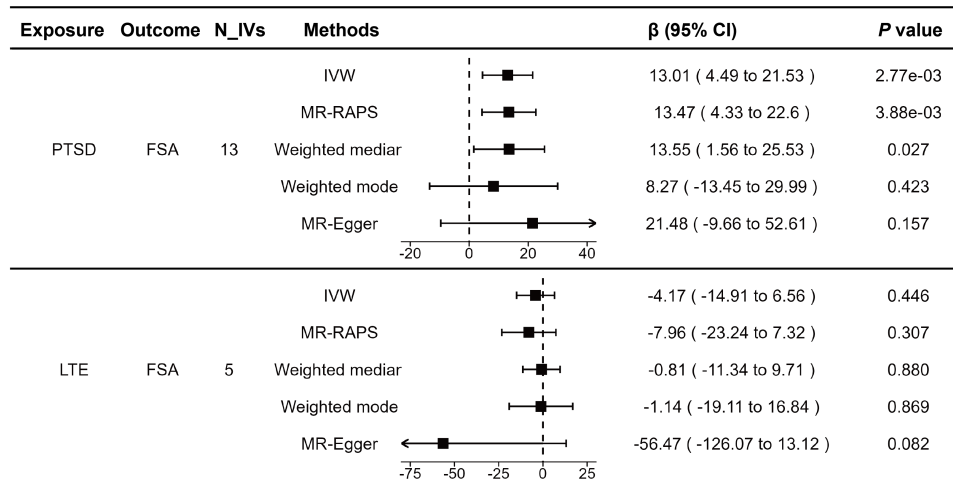


Fig. 5 MR estimates of PTSD and LTE on FSA. Data are presented as β and 95% CI. N_IVs: the number of instrument variants. Abbreviations: PTSD, post-traumatic stress disorder; LTE, lifetime trauma events; FSA, frontal poles surface area.

381 informed analyses to investigate the genetic association between PTSD and the
 382 brain structures of trauma-related neural circuits, using LTE as control. Our findings
 383 revealed varying degrees of relationship between PTSD and brain structures related
 384 to trauma circuits using different methods. These results provide new genetic evidence
 385 for PTSD and a deeper perspective into the pathogenesis.

386 Previous findings in animal studies and neuroimaging research regarding neural
 387 circuitry have been similarly corroborated on a genetic level. We have discovered
 388 genetic correlations or overlaps between PTSD and these brain regions at various
 389 levels. Additionally, previous studies have shown that there is a strong correlation
 390 between PTSD and LTE in both twin studies and genetic correlation studies.[44, 77]
 391 For most traits about mental health, r_g with PTSD was also quite similar to r_g with
 392 LTE[44]. In our analysis, there were more significant or stronger results for PTSD than
 393 LTE, indicating that trauma-related neural circuits were more related to the onset of
 394 PTSD than to the mediating effect of PTSD caused by being related to LTE. This
 395 further underscores the significance of neural circuits in PTSD.

396 We found that the heritability of SNPs associated with PTSD was significantly
 397 enriched in GTEx v8 “Brain Anterior cingulate cortex (BA24)”, “Brain Frontal Cortex
 398 (BA9)” and “Brain Cortex”, while there was no obvious founding in the SNPs of LTE.
 399 BA 24 is the ventral part of the brain anterior cingulate, which is connected with the
 400 amygdala and hippocampus, and it is involved in emotional tasks such as assessing
 401 the salience of emotion and motivational information.[78] BA9 is a cellularly defined
 402 part of the frontal cortex, and it is involved in short-term memory, suppressing sadness
 403 and recall which may be associated with the onset of PTSD.[79–81] These regions
 404 are anatomically close to the mPFC and its connections to the subcortex. The brain
 405 cortex covers a wider scope, involving attention, perception, consciousness, thinking,

memory, and many other aspects. This suggests that the association of PTSD with its 406
neural circuitry can indeed be explained at the genetic level. This provided a reference 407
for our subsequent research on the cortex. 408

We studied the global and local genetic correlation between trauma-related traits 409
and brain structure-related traits and found a weak global correlation between PTSD 410
and GSA, although the results failed to pass FDR. Furthermore, we thought this 411
might be due to mixed effect directions between the two traits. This was also con- 412
firmed in the subsequent LAVA local correlations and polygenic overlap results. Apart 413
from FTH, we found 33 significant local bivariate correlations in 8 other pairs about 414
PTSD. LAVA analysis showed a balanced mixture of concordant and discordant 415
results throughout the genome. This suggested that different loci might be involved in 416
different processes between disease and neurological traits, leading to different direc- 417
tions of influence. It was worth noting that the region in chr7:155280611-156344386 418
or chr17:43460501-4486583 was significant in both pairs about PTSD; the latter also 419
coincided with the conjFDR results. Genes in these loci might play an important role 420
in the genetic association between PTSD and brain structure traits. 421

We found that the trauma-related traits were considerably more polygenic (7.8K– 422
10K) than brain structure (0.3K–3.1K), reflecting that the mechanism of genetic 423
factors in PTSD and LTE was far more complex than the mechanism in brain struc- 424
ture. LDSC was also used in MiXeR to estimate global correlation. In the previous 425
part, when calculating global correlations, we used SNPs in HAPMAP3, and there was 426
no obvious difference from the results calculated here. The results of bivariate MiXeR 427
revealed that the genetic overlap between PTSD and brain structure accounts for at 428
least 77%, some of these results were further supported by AIC values. Combining 429
with the mixing effects we found in the conjFDR results, we inferred that there was 430
genetic overlap without correlation[40] for PTSD and brain structure traits. 431

Through novelty search and functional annotation of 40 PTSD risk loci identified 432
by conjFDR, we studied the possible mechanisms of PTSD and structural changes in 433
neural circuits. 3p21.31 (lead SNP rs2352974) was a novel locus and was associated in 434
both CG and UNC with PTSD. It was mapped to *TRAIP* positionally and to RBM6 435
and RNF123 by eQTL in the brain. The *TRAIP* gene is linked to the processes of 436
DNA damage and repair.[82, 83] Specifically, *TRAIP* functions in the disentanglement 437
of stalled replication forks during mitosis, thereby mitigating the occurrence of DNA 438
bridges and premature loss of neural stem cells[84], so the damage to white matter 439
in PTSD patients might be related to their neuron count. RBM6 and *TRAIP* have 440
similar functions and are involved in the repair of DNA damage.[85] *RNF123* is linked 441
to the ubiquitin-proteasome system and plays a role in depression.[86]. This process 442
was confirmed in the gene-set analysis related to UNC, indicating that it was likely to 443
be involved in the process of white matter damage in PTSD patients. 444

After annotating candidate genes from conjFDR results onto the genome using 445
three methods, three genes (*MAPT-AS1*, *SPPL2C*, and *CRHR1*) were identified across 446
5 or more pairs, all of which are located on chromosome 17. Moreover, in this area, the 447
conjFDR results of PTSD-GSA and PTSD-FST were consistent with the local corre- 448
lation results of LAVA. *MAPT* is the gene responsible for encoding tau protein, which 449

450 plays an important role in neurodegenerative diseases such as AD. The primary deposi-
451 tion sites for tau protein are the hippocampus and frontal lobe, precisely aligning with
452 neural circuits implicated in trauma-related processes.[87, 88] *SPPL2C* is in the region
453 of *MAPT*, is associated with *MAPT* expression in astrocytes.[89]. It has been observed
454 that *CRHR1* antagonists can inhibit the activation of the CRH/NF- κ B/BDNF path-
455 way, thereby effectively preventing the rapid loss of synapses and memory impairment
456 associated with trauma-induced delirium-like syndrome.[90] This may provide a new
457 hypothesis for the occurrence of PTSD.

458 However, our research still has some limitations. First, there may be some trauma
459 subjects might also be included in the neuroimaging samples, but we were unable
460 to ascertain the influence of such overlap on our findings. Second, compared to
461 schizophrenia[91] and bipolar disorder[92], PTSD exhibits lower heritability[93], so
462 we have identified fewer loci associated with each phenotype in our study. And the
463 summary we used exclusively focused on individuals of European ancestry. This lim-
464 ited scope may not fully capture the entirety of the genetic etiology involved. Future
465 investigations may necessitate larger GWAS cohorts, encompassing diverse popula-
466 tion groups, to corroborate our findings comprehensively. Then, the traits we selected
467 mainly focused on the structure of the neural circuits rather than function. Some
468 studies believe that PTSD is a disease caused by abnormal brain neural circuits.[15]
469 Although there are GWAS on functional imaging, the phenotypic selection in these
470 studies was derived through independent component analysis (ICA).[94] Consequently,
471 the integration of phenotypes with neural circuits is challenging due to this cho-
472 sen methodology. Last, we were unable to ascertain the causal relationship between
473 trauma-related traits and brain structural traits, indicating the need for further
474 research in this regard.

475 5 Conclusion

476 In this study, we have presented evidence of polygenic overlap between PTSD and
477 trauma-related neural circuits. Forty overlapping loci and 1,426 genes were identified
478 among nine phenotypes associated with brain structure in the context of PTSD. These
479 findings contribute valuable insights into the shared genetic architecture between
480 PTSD and its neural circuits, suggesting a common neurobiological foundation.

481 **Supplementary information.** Supplementary data to this article can be found at
482 [Supplementary material](#) and [Supplementary tables](#).

483 **Acknowledgements.** We express our gratitude to Professor Adam X. Maihofer for
484 providing the GWAS summary data on PTSD and LTE. We also express our gratitude
485 to the ENIGMA and Professor Bingxin Zhao et al. for their foundational research in
486 the brain structural GWAS. The numerical calculations in this paper have been done
487 on the supercomputing system in the Supercomputing Center of Wuhan University.

Declarations

488

- Funding: This work was supported by grants from the National Natural Science Foundation of China (U21A20364) and the National Key R&D Program of China (2018YFC1314600). 489 490 491
- Conflict of interest: All authors declare that they have no competing interests. 492
- Ethics approval and consent to participate: All GWAS data sets included in this study were approved by the relevant ethics committees, and informed consent was obtained from all participants. 493 494 495
- Consent for publication: Not applicable 496
- Data availability: The PTSD GWAS data, encompassing the queues of both the PGC and the UK Biobank, were obtained through direct correspondence with the original authors.[44], and PTSD GWAS data from MVP and FinnGen can be respectively accessed at [https://www.research.va.gov/mvp/\(dbGaP Study Accession phs001672\)](https://www.research.va.gov/mvp/(dbGaP%20Study%20Accession%20phs001672)) and <https://www.finnngen.fi/en>. The cortical and subcortical GWAS data were obtained from <https://enigma.ini.usc.edu/>, and the white matter GWAS data was from <https://zenodo.org/records/4549730>. 497 498 499 500 501 502 503
- Materials availability: Not applicable 504
- Code availability: All software used to conduct the analyses in this paper are freely available online: METAL: <https://github.com/statgen/METAL>. LDSC and LDSC-SEG: <https://github.com/bulik/ldsc>, LAVA: <https://github.com/josefin-werme/LAVA>, MiXeR: <https://github.com/precimed/mixer>, pleiofdr: <https://github.com/precimed/pleiofdr>, FUMA: <https://fuma.ctglab.nl/>. 505 506 507 508 509
- Author contribution: **Qian Gong** (Data curation, Formal analysis, Investigation, Methodology, Visualization, Writing original draft). **Honggang Lv** (Data curation, Formal analysis, Methodology, Editing). **Lijun Kang** (Investigation, Editing). **Simeng Ma** (Data curation, Investigation). **Nan Zhang** (Investigation). **Xinhui Xie** (Investigation, Editing). **Enqi Zhou** (Investigation). **Zipeng Deng** (Investigation). **Jiwei Liu** (Data curation, Formal analysis, Methodology, Editing). **Zhongchun Liu** (Methodology, Investigation, Resources, Supervision, Editing). 510 511 512 513 514 515 516

References

- [1] Pai, A., Suris, A. M. & North, C. S. Posttraumatic Stress Disorder in the DSM-5: Controversy, Change, and Conceptual Considerations. *Behav Sci (Basel)* **7**, 7 (2017).
- [2] Shalev, A., Liberzon, I. & Marmar, C. Post-Traumatic Stress Disorder. *N Engl J Med* **376**, 2459–2469 (2017).
- [3] McLaughlin, K. A. *et al.* Subthreshold posttraumatic stress disorder in the world health organization world mental health surveys. *Biol Psychiatry* **77**, 375–384 (2015).
- [4] Kessler, R. C. & Wang, P. S. The descriptive epidemiology of commonly occurring mental disorders in the United States. *Annu Rev Public Health* **29**, 115–129

(2008).

- [5] Kilpatrick, D. G. *et al.* National estimates of exposure to traumatic events and PTSD prevalence using DSM-IV and DSM-5 criteria. *J Trauma Stress* **26**, 537–547 (2013).
- [6] Maddox, S. A., Hartmann, J., Ross, R. A. & Ressler, K. J. Deconstructing the Gestalt: Mechanisms of Fear, Threat, and Trauma Memory Encoding. *Neuron* **102**, 60–74 (2019).
- [7] Milad, M. R. *et al.* Neurobiological basis of failure to recall extinction memory in posttraumatic stress disorder. *Biol Psychiatry* **66**, 1075–1082 (2009).
- [8] Iqbal, J., Huang, G.-D., Xue, Y.-X., Yang, M. & Jia, X.-J. The neural circuits and molecular mechanisms underlying fear dysregulation in posttraumatic stress disorder. *Front Neurosci* **17**, 1281401 (2023).
- [9] Rauch, S. L., Shin, L. M. & Phelps, E. A. Neurocircuitry models of posttraumatic stress disorder and extinction: Human neuroimaging research—past, present, and future. *Biol Psychiatry* **60**, 376–382 (2006).
- [10] Harnett, N. G., Goodman, A. M. & Knight, D. C. PTSD-related neuroimaging abnormalities in brain function, structure, and biochemistry. *Exp Neurol* **330**, 113331 (2020).
- [11] Krabbe, S., Gründemann, J. & Lüthi, A. Amygdala Inhibitory Circuits Regulate Associative Fear Conditioning. *Biol Psychiatry* **83**, 800–809 (2018).
- [12] Tovote, P., Fadok, J. P. & Lüthi, A. Neuronal circuits for fear and anxiety. *Nat Rev Neurosci* **16**, 317–331 (2015).
- [13] Asede, D., Bosch, D., Lüthi, A., Ferraguti, F. & Ehrlich, I. Sensory inputs to intercalated cells provide fear-learning modulated inhibition to the basolateral amygdala. *Neuron* **86**, 541–554 (2015).
- [14] Dejean, C. *et al.* Neuronal Circuits for Fear Expression and Recovery: Recent Advances and Potential Therapeutic Strategies. *Biol Psychiatry* **78**, 298–306 (2015).
- [15] Patel, R., Spreng, R. N., Shin, L. M. & Girard, T. A. Neurocircuitry models of posttraumatic stress disorder and beyond: A meta-analysis of functional neuroimaging studies. *Neurosci Biobehav Rev* **36**, 2130–2142 (2012).
- [16] Hayes, J. P., Hayes, S. M. & Mikedis, A. M. Quantitative meta-analysis of neural activity in posttraumatic stress disorder. *Biol Mood Anxiety Disord* **2**, 9 (2012).
- [17] Qin, C. *et al.* Dorsal Hippocampus to Infralimbic Cortex Circuit is Essential for the Recall of Extinction Memory. *Cereb Cortex* **31**, 1707–1718 (2021).

- [18] Cleren, C. *et al.* Low-frequency stimulation of the ventral hippocampus facilitates extinction of contextual fear. *Neurobiol Learn Mem* **101**, 39–45 (2013).
- [19] Guan, Y., Chen, X., Zhao, B., Shi, Y. & Han, F. What Happened in the Hippocampal Axon in a Rat Model of Posttraumatic Stress Disorder. *Cell Mol Neurobiol* **42**, 723–737 (2022).
- [20] Hayes, J. P. *et al.* Reduced hippocampal and amygdala activity predicts memory distortions for trauma reminders in combat-related PTSD. *J Psychiatr Res* **45**, 660–669 (2011).
- [21] Carrión, V. G., Haas, B. W., Garrett, A., Song, S. & Reiss, A. L. Reduced hippocampal activity in youth with posttraumatic stress symptoms: An fMRI study. *J Pediatr Psychol* **35**, 559–569 (2010).
- [22] Do-Monte, F. H., Quiñones-Laracuente, K. & Quirk, G. J. A temporal shift in the circuits mediating retrieval of fear memory. *Nature* **519**, 460–463 (2015).
- [23] Do-Monte, F. H., Manzano-Nieves, G., Quiñones-Laracuente, K., Ramos-Medina, L. & Quirk, G. J. Revisiting the role of infralimbic cortex in fear extinction with optogenetics. *J Neurosci* **35**, 3607–3615 (2015).
- [24] Garfinkel, S. N. *et al.* Impaired contextual modulation of memories in PTSD: An fMRI and psychophysiological study of extinction retention and fear renewal. *J Neurosci* **34**, 13435–13443 (2014).
- [25] Aupperle, R. L. *et al.* Dorsolateral prefrontal cortex activation during emotional anticipation and neuropsychological performance in posttraumatic stress disorder. *Arch Gen Psychiatry* **69**, 360–371 (2012).
- [26] Rougemont-Bücking, A. *et al.* Altered processing of contextual information during fear extinction in PTSD: An fMRI study. *CNS Neurosci Ther* **17**, 227–236 (2011).
- [27] Nicholson, A. A. *et al.* The Dissociative Subtype of Posttraumatic Stress Disorder: Unique Resting-State Functional Connectivity of Basolateral and Centromedial Amygdala Complexes. *Neuropsychopharmacology* **40**, 2317–2326 (2015).
- [28] Gilmartin, M. R., Balderston, N. L. & Helmstetter, F. J. Prefrontal cortical regulation of fear learning. *Trends Neurosci* **37**, 455–464 (2014).
- [29] Harnett, N. G., Ference, E. W., Knight, A. J. & Knight, D. C. White matter microstructure varies with post-traumatic stress severity following medical trauma. *Brain Imaging Behav* **14**, 1012–1024 (2020).
- [30] Koch, S. B. J. *et al.* Decreased uncinate fasciculus tract integrity in male and female patients with PTSD: A diffusion tensor imaging study. *J Psychiatry Neurosci* **42**, 331–342 (2017).

- [31] Molnár, Z. *et al.* New insights into the development of the human cerebral cortex. *J Anat* **235**, 432–451 (2019).
- [32] Batouli, S. A. H., Trollor, J. N., Wen, W. & Sachdev, P. S. The heritability of volumes of brain structures and its relationship to age: A review of twin and family studies. *Ageing Res Rev* **13**, 1–9 (2014).
- [33] Batouli, S. A. H. *et al.* Heritability of brain volumes in older adults: The Older Australian Twins Study. *Neurobiol Aging* **35**, 937.e5–18 (2014).
- [34] Kanchibhotla, S. C. *et al.* Genetics of ageing-related changes in brain white matter integrity - a review. *Ageing Res Rev* **12**, 391–401 (2013).
- [35] Grasby, K. L. *et al.* The genetic architecture of the human cerebral cortex. *Science* **367**, eaay6690 (2020).
- [36] Satizabal, C. L. *et al.* Genetic architecture of subcortical brain structures in 38,851 individuals. *Nat Genet* **51**, 1624–1636 (2019).
- [37] Hibar, D. P. *et al.* Novel genetic loci associated with hippocampal volume. *Nat Commun* **8**, 13624 (2017).
- [38] Zhao, B. *et al.* Common genetic variation influencing human white matter microstructure. *Science* **372**, eabf3736 (2021).
- [39] Stauffer, E.-M. *et al.* The genetic relationships between brain structure and schizophrenia. *Nat Commun* **14**, 7820 (2023).
- [40] Cheng, W. *et al.* Shared genetic architecture between schizophrenia and subcortical brain volumes implicates early neurodevelopmental processes and brain development in childhood. *Mol Psychiatry* **27**, 5167–5176 (2022).
- [41] Wu, B.-S. *et al.* Genome-wide association study of cerebellar white matter microstructure and genetic overlap with common brain disorders. *Neuroimage* **269**, 119928 (2023).
- [42] Shang, M.-Y. *et al.* Genetic associations between bipolar disorder and brain structural phenotypes. *Cereb Cortex* bhad014 (2023).
- [43] Ressler, K. J. *et al.* Post-traumatic stress disorder: Clinical and translational neuroscience from cells to circuits. *Nat Rev Neurol* **18**, 273–288 (2022).
- [44] Maihofer, A. X. *et al.* Enhancing Discovery of Genetic Variants for Posttraumatic Stress Disorder Through Integration of Quantitative Phenotypes and Trauma Exposure Information. *Biol Psychiatry* **91**, 626–636 (2022).
- [45] Nievergelt, C. M. *et al.* International meta-analysis of PTSD genome-wide association studies identifies sex- and ancestry-specific genetic risk loci. *Nat Commun*

- 10**, 4558 (2019).
- [46] Frei, O. *et al.* Bivariate causal mixture model quantifies polygenic overlap between complex traits beyond genetic correlation. *Nat Commun* **10**, 2417 (2019).
- [47] Smeland, O. B. *et al.* Discovery of shared genomic loci using the conditional false discovery rate approach. *Hum Genet* **139**, 85–94 (2020).
- [48] Watanabe, K., Taskesen, E., van Bochoven, A. & Posthuma, D. Functional mapping and annotation of genetic associations with FUMA. *Nat Commun* **8**, 1826 (2017).
- [49] Stein, M. B. *et al.* Genome-wide association analyses of post-traumatic stress disorder and its symptom subdomains in the Million Veteran Program. *Nat Genet* **53**, 174–184 (2021).
- [50] Harrington, K. M. *et al.* Validation of an Electronic Medical Record-Based Algorithm for Identifying Posttraumatic Stress Disorder in U.S. Veterans. *J Trauma Stress* **32**, 226–237 (2019).
- [51] Willer, C. J., Li, Y. & Abecasis, G. R. METAL: Fast and efficient meta-analysis of genomewide association scans. *Bioinformatics* **26**, 2190–2191 (2010).
- [52] Desikan, R. S. *et al.* An automated labeling system for subdividing the human cerebral cortex on MRI scans into gyral based regions of interest. *Neuroimage* **31**, 968–980 (2006).
- [53] Rakic, P. Specification of cerebral cortical areas. *Science* **241**, 170–176 (1988).
- [54] Brodmann, K. Vergleichende lokalisationslehre der grosshirnrinde. *Leipzig: Barth JA* (1905).
- [55] Patenaude, B., Smith, S. M., Kennedy, D. N. & Jenkinson, M. A Bayesian model of shape and appearance for subcortical brain segmentation. *Neuroimage* **56**, 907–922 (2011).
- [56] Fischl, B. *et al.* Whole brain segmentation: Automated labeling of neuroanatomical structures in the human brain. *Neuron* **33**, 341–355 (2002).
- [57] Grieve, S. M., Williams, L. M., Paul, R. H., Clark, C. R. & Gordon, E. Cognitive aging, executive function, and fractional anisotropy: A diffusion tensor MR imaging study. *AJNR Am J Neuroradiol* **28**, 226–235 (2007).
- [58] Finucane, H. K. *et al.* Heritability enrichment of specifically expressed genes identifies disease-relevant tissues and cell types. *Nat Genet* **50**, 621–629 (2018).
- [59] GTEx Consortium. The GTEx Consortium atlas of genetic regulatory effects across human tissues. *Science* **369**, 1318–1330 (2020).

- [60] Bulik-Sullivan, B. *et al.* An atlas of genetic correlations across human diseases and traits. *Nat Genet* **47**, 1236–1241 (2015).
- [61] 1000 Genomes Project Consortium *et al.* A global reference for human genetic variation. *Nature* **526**, 68–74 (2015).
- [62] Werme, J., van der Sluis, S., Posthuma, D. & de Leeuw, C. A. An integrated framework for local genetic correlation analysis. *Nat Genet* **54**, 274–282 (2022).
- [63] Andreassen, O. A. *et al.* Improved detection of common variants associated with schizophrenia and bipolar disorder using pleiotropy-informed conditional false discovery rate. *PLoS Genet* **9**, e1003455 (2013).
- [64] Buniello, A. *et al.* The NHGRI-EBI GWAS Catalog of published genome-wide association studies, targeted arrays and summary statistics 2019. *Nucleic Acids Res* **47**, D1005–D1012 (2019).
- [65] Rentzsch, P., Witten, D., Cooper, G. M., Shendure, J. & Kircher, M. CADD: Predicting the deleteriousness of variants throughout the human genome. *Nucleic Acids Res* **47**, D886–D894 (2019).
- [66] Boyle, A. P. *et al.* Annotation of functional variation in personal genomes using RegulomeDB. *Genome Res* **22**, 1790–1797 (2012).
- [67] Roadmap Epigenomics Consortium *et al.* Integrative analysis of 111 reference human epigenomes. *Nature* **518**, 317–330 (2015).
- [68] GTEx Consortium *et al.* Genetic effects on gene expression across human tissues. *Nature* **550**, 204–213 (2017).
- [69] Wang, D. *et al.* Comprehensive functional genomic resource and integrative model for the human brain. *Science* **362**, eaat8464 (2018).
- [70] Burgess, S., Thompson, S. G. & CRP CHD Genetics Collaboration. Avoiding bias from weak instruments in Mendelian randomization studies. *Int J Epidemiol* **40**, 755–764 (2011).
- [71] Kamat, M. A. *et al.* PhenoScanner V2: An expanded tool for searching human genotype-phenotype associations. *Bioinformatics* **35**, 4851–4853 (2019).
- [72] Myers, T. A., Chanock, S. J. & Machiela, M. J. LDlinkR: An R Package for Rapidly Calculating Linkage Disequilibrium Statistics in Diverse Populations. *Front Genet* **11**, 157 (2020).
- [73] Burgess, S. *et al.* Using published data in Mendelian randomization: A blueprint for efficient identification of causal risk factors. *Eur J Epidemiol* **30**, 543–552 (2015).

- [74] Bowden, J., Davey Smith, G., Haycock, P. C. & Burgess, S. Consistent Estimation in Mendelian Randomization with Some Invalid Instruments Using a Weighted Median Estimator. *Genet Epidemiol* **40**, 304–314 (2016).
- [75] Bowden, J., Davey Smith, G. & Burgess, S. Mendelian randomization with invalid instruments: Effect estimation and bias detection through Egger regression. *Int J Epidemiol* **44**, 512–525 (2015).
- [76] Verbanck, M., Chen, C.-Y., Neale, B. & Do, R. Detection of widespread horizontal pleiotropy in causal relationships inferred from Mendelian randomization between complex traits and diseases. *Nat Genet* **50**, 693–698 (2018).
- [77] Stein, M. B., Jang, K. L., Taylor, S., Vernon, P. A. & Livesley, W. J. Genetic and environmental influences on trauma exposure and posttraumatic stress disorder symptoms: A twin study. *Am J Psychiatry* **159**, 1675–1681 (2002).
- [78] Bush, G., Luu, P. & Posner, M. I. Cognitive and emotional influences in anterior cingulate cortex. *Trends Cogn Sci* **4**, 215–222 (2000).
- [79] Babiloni, C. *et al.* Human cortical responses during one-bit delayed-response tasks: An fMRI study. *Brain Res Bull* **65**, 383–390 (2005).
- [80] Kaur, S. *et al.* Cingulate cortex anatomical abnormalities in children and adolescents with bipolar disorder. *Am J Psychiatry* **162**, 1637–1643 (2005).
- [81] Tulving, E. *et al.* Neuroanatomical correlates of retrieval in episodic memory: Auditory sentence recognition. *Proc Natl Acad Sci U S A* **91**, 2012–2015 (1994).
- [82] Wu, R. A. *et al.* TRAIP is a master regulator of DNA interstrand crosslink repair. *Nature* **567**, 267–272 (2019).
- [83] Wu, R. A., Pellman, D. S. & Walter, J. C. The Ubiquitin Ligase TRAIP: Double-Edged Sword at the Replisome. *Trends Cell Biol* **31**, 75–85 (2021).
- [84] O’Neill, R. S. & Rusan, N. M. Traip controls mushroom body size by suppressing mitotic defects. *Development* **149**, dev199987 (2022).
- [85] Awwad, S. W., Darawshe, M. M., Machour, F. E., Arman, I. & Ayoub, N. Recruitment of RBM6 to DNA Double-Strand Breaks Fosters Homologous Recombination Repair. *Mol Cell Biol* **43**, 130–142 (2023).
- [86] Teyssier, J.-R., Rey, R., Ragot, S., Chauvet-Gelinier, J.-C. & Bonin, B. Correlative gene expression pattern linking RNF123 to cellular stress-senescence genes in patients with depressive disorder: Implication of DRD1 in the cerebral cortex. *J Affect Disord* **151**, 432–438 (2013).
- [87] Strang, K. H., Golde, T. E. & Giasson, B. I. MAPT mutations, tauopathy, and mechanisms of neurodegeneration. *Lab Invest* **99**, 912–928 (2019).

- [88] Leveille, E., Ross, O. A. & Gan-Or, Z. Tau and MAPT genetics in tauopathies and synucleinopathies. *Parkinsonism Relat Disord* **90**, 142–154 (2021).
- [89] He, L. *et al.* Exome-wide age-of-onset analysis reveals exonic variants in ERN1 and SPPL2C associated with Alzheimer’s disease. *Transl Psychiatry* **11**, 146 (2021).
- [90] Cursano, S. *et al.* A CRHR1 antagonist prevents synaptic loss and memory deficits in a trauma-induced delirium-like syndrome. *Mol Psychiatry* **26**, 3778–3794 (2021).
- [91] Trubetskoy, V. *et al.* Mapping genomic loci implicates genes and synaptic biology in schizophrenia. *Nature* **604**, 502–508 (2022).
- [92] Stahl, E. A. *et al.* Genome-wide association study identifies 30 loci associated with bipolar disorder. *Nat Genet* **51**, 793–803 (2019).
- [93] Nievergelt, C. M. *et al.* Discovery of 95 PTSD loci provides insight into genetic architecture and neurobiology of trauma and stress-related disorders. *medRxiv* 2023.08.31.23294915 (2023).
- [94] Zhao, B. *et al.* Common variants contribute to intrinsic human brain functional networks. *Nat Genet* **54**, 508–517 (2022).